

## **PHYSICALLY BASED SEISMIC HAZARD ASSESSMENT FOR EGYPT AND ITS IMPLICATION ON CRITICAL STRUCTURES**

M.N.ELGABRY<sup>1,2,\*</sup>, H.M. HASSAN<sup>1,2,3</sup>, F.ROMANELLI<sup>2</sup>, G.F. PANZA<sup>4,5,6</sup>

<sup>1</sup> *National Research Institute of Astronomy and Geophysics, 11421 Helwan, Cairo, Egypt (Affiliation ID: 60030681).*

<sup>2</sup> *Department of Mathematics and Geosciences, Via Weiss 4, I-34127, Trieste, Italy.*

<sup>3</sup> *North Africa Group for Earthquakes and Tsunami Studies (NAGET), Ne t40/OEA ICTP, Italy.*

<sup>4</sup> *Institute of Geophysics, China Earthquake Administration, Beijing, China.*

<sup>5</sup> *International Seismic Safety Organization (ISSO) - [www.issquake.org](http://www.issquake.org).*

<sup>6</sup> *Accademia Nazionale dei Lincei, Roma, Italy.*

*\*E-mail contact of main author:*

### **Abstract**

Seismic hazard studies in Egypt have gone through several stages of development that included incorporation of new data and adoption of new methods. In this study, we provide an update of the seismic hazard maps available for Egypt that incorporates revised historical earthquake catalogs, morphostructural zonation data (MZ), revised focal mechanism solutions and mechanical models of the lithospheric structure. This is done within the framework of the neo-deterministic seismic hazard assessment (NDSHA) procedure that may efficiently incorporate earthquake source rupture data, geological information and any reliable new information to adequately compute the earthquake ground motion maps, like PGA, PGV, and PGD. NDSHA provides an opportunity to comprehensively generate ground acceleration records where a substantial challenge of lacking recorded data. To consistently assess the uncertainty of our understanding of the seismic hazard in Egypt and its effect on critical structures a sensitivity analysis is performed varying (a) source focal mechanism, (b) directivity (c) rupture process and (d) seismotectonic model.

**Key Words:** site-specific seismic hazard; Suez Canal; NDSHA; Seismic Input

### **1. Introduction**

The Suez Canal Corridor Area Project is a mega project in Egypt that was launched on 5 August 2014. The project aims to increase the role of the Suez Canal region in international trading and to develop the three canal main cities: Suez, Ismailia, and Port Said and connects them with the Sinai Peninsula. In addition, the project involves constructing a new city (new Ismailia city), an industrial zone, fish farms, completing the technology valley, expanding five existing ports, digging a new canal parallel to the Suez Canal, and building four new tunnels between Suez Canal cities and Sinai. The proposed four tunnels will be dug to connect the Sinai Peninsula to the Egyptian homeland. Two tunnels under construction in Port Said and another two in Ismailia (Fig.1). The proper design of such strategic structures requires efficient and reliable computation of seismic hazard in order to provide the seismic input at the site of the tunnel in Ismailia needed for the engineering studies for the structural assessment and non-linear behavior of the soil analysis.

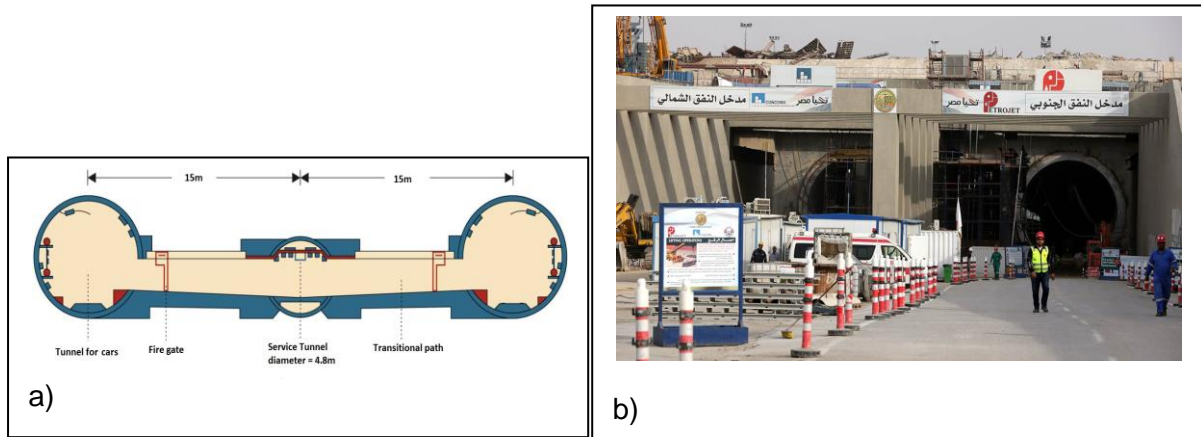


Fig.1 Ismailia first tunnel. a) a cross section of the tunnel; b) the tunnel during construction.

Seismic hazard assessment for a given site (site-specific seismic hazard) can be carried out using empirical or physics-based methods. Seismic hazard assessment that relies on physics-based models should be encouraged when dealing with infrastructure and strategic buildings. This method employs numerical modeling codes based upon the physical parameterization of fault rupture process and seismic wave propagation to reliably predict the ground motion parameters at different geographic scales and levels of details.

In this study and following the Neo-deterministic seismic hazard assessment (NDSHA) method, we define the Maximum Credible Seismic Input (MCSI) at the site of Ismailia tunnel at two levels of details (Fasan et al., 2017), both to be used as reliable seismic input by the structural and geotechnical engineers. The first level of detail provides the “Maximum Credible Seismic Input at bedrock” ( $MCSI_{BD}$ ), deliberately ignoring the “so-called” site-effects that, due to the tensor nature of earthquake ground motions, are not persistent but strongly dependent on the source process, and the transmitting (pathway) medium (Molchan et. Al., 2011 and Hassan et al., 2017). At this level, we use the same input data used in Hassan et al., (2017) to compute the  $MCSI_{BD}$  at the site of the tunnel. In the second level of detail, the Regional Scale Analysis (RSA) is used as a reference to select the most dangerous sources for the site and ground motion parameter of interest. As for these sources, a detailed Site-Specific Analysis (SSA), which considers the local structural properties, is then carried out for each pathway as described in the next section. The SSA is a prerequisite to determine the “Maximum Credible Seismic Site Specific Input” ( $MCSI_{SS}$ ).

## 2. Methodology

The Neo Deterministic Seismic Hazard Assessment (NDSHA) (Panza et al., 2001; 2012 and its update in Magrin et al., 2016) is a scenario-based procedure which supplies realistic time

history ground motions, which are calculated as the tensor product of the earthquake source and the Green's function of the medium, thus preserving the tensor nature of the physical problem (Fig.2). NDSHA computation is based on the maximum magnitudes occurred within sources that may affect the studied site regardless of their rate of occurrence. Very realistic synthetic seismograms, calibrated against experimental records whenever possible, can be computed from the knowledge of the earthquake rupture process and of the inelastic pathway mechanical properties. The computed seismograms supply reliable estimates of engineering relevant parameters such as peak ground motion parameters and the maximum credible seismic input (MCSI) (Fasan et al., 2015; Fasan 2017). The seismograms computed at the site of interest can be used immediately as input for the Non-Linear Time History Analysis of any built structure without any further processing (e.g., filtering or scaling). In fact, realistic time histories are of a great importance for structural and technical engineers willing to design a new structure and/or evaluate the seismic performance of the existing built environment and to investigate the non-linear behavior of soil at the site of interest.

At the national scale, NDSHA makes use of information about the spatial distribution of large magnitude earthquakes, as defined by seismic history and seismotectonics and an extensive set of relevant geological and geophysical data (Zuccolo et al., 2011). The basic product of this method is a map in which the maximum of a given ground motion parameter - peak ground acceleration (PGA), velocity (PGV) and displacement (PGD) - or any other parameter relevant to seismic engineering, which can be extracted from the computed seismograms, is associated to each site. This kind of map, which is really effective for engineering purposes, does not provide any information about the recurrence ("return period") of the events, thus does not require any assumption on the probability model of earthquakes occurrence (e.g. not validated Poissonian model assumption); information is provided only in terms of *average occurrence rates*. The transformation of (necessarily rough) average occurrence rates into "probabilities" is willingly avoided. Clearly, including additional temporal information, which is very uncertain, increases uncertainties in the resulting estimates and thus it should be considered only if and when strictly necessary. We believe that the engineering use of these average occurrence rates is questionable, and do not suggest their use.

The NDSHA procedure is very flexible and can be enhanced easily: the computer codes are constantly improved by incorporating all relevant progress in the knowledge of the physics of geological processes and in their numerical modeling.

Each seismogenic source in NDSHA at national or regional scale is arbitrarily placed at the center of a  $0.2^\circ \times 0.2^\circ$  cell of a regular grid that covers the study region, and we call it cellular source. Each cellular source is modeled as a scaled point-source and is characterized by focal

mechanism and earthquake magnitude. Cellular sources are defined taking into account the available information, as provided by the seismotectonic model, the morphostructural zonation and reported seismicity. Namely, the location of possible future earthquakes is constrained by the seismogenic zones and by the seismogenic nodes. In the first step of cellular sources definition (discretization), earthquake epicenters reported in the catalog are grouped into  $0.2^\circ \times 0.2^\circ$  cells, and to each cell, the maximum magnitude recorded within it is assigned. A smoothing window is then applied, so that earthquake magnitudes are copied in the neighboring cells, and the maximum magnitude source for each cell is retained (smoothing). The smoothing procedure is basically needed for handling the uncertainty associated with the localization of the source and the linear physical dimension of the source often exceeds the linear dimension of a cell (which is typically  $0.2^\circ \times 0.2^\circ$ ).

The cellular sources that lie in a seismogenic zone are selected among the ones defined during the smoothing process and, if the resulting magnitude in each cell is lower than 5, a magnitude five is assigned by default. This selection is mainly based on the hypothesis that, wherever a seismogenic zone is defined, damaging earthquakes may occur, and the value of 5 is conventionally taken as the lower bound for the magnitude of moderate damaging earthquakes (<http://www.geo.mtu.edu/UPSeis/magnitude.html>). Seismogenic nodes are earthquake-prone areas identified through morphostructural analysis. For the Egyptian territory, the identification of the seismogenic nodes has been performed by Hassan et al. (2016). The nodes have been defined as circles of radius  $R = 20$  km centered at points of intersection of lineaments. Such dimension is comparable with the size of a seismic source, which can generate damaging events. A magnitude threshold of 5 have been considered for the estimation of the seismic potential of the node through the pattern recognition technique. A double-couple point source is located at the center of each cell, assigning a focal mechanism consistent with the properties of the corresponding seismogenic zone or seismogenic node. If a cell belongs to a seismogenic zone and a seismogenic node, we consider both focal mechanisms.

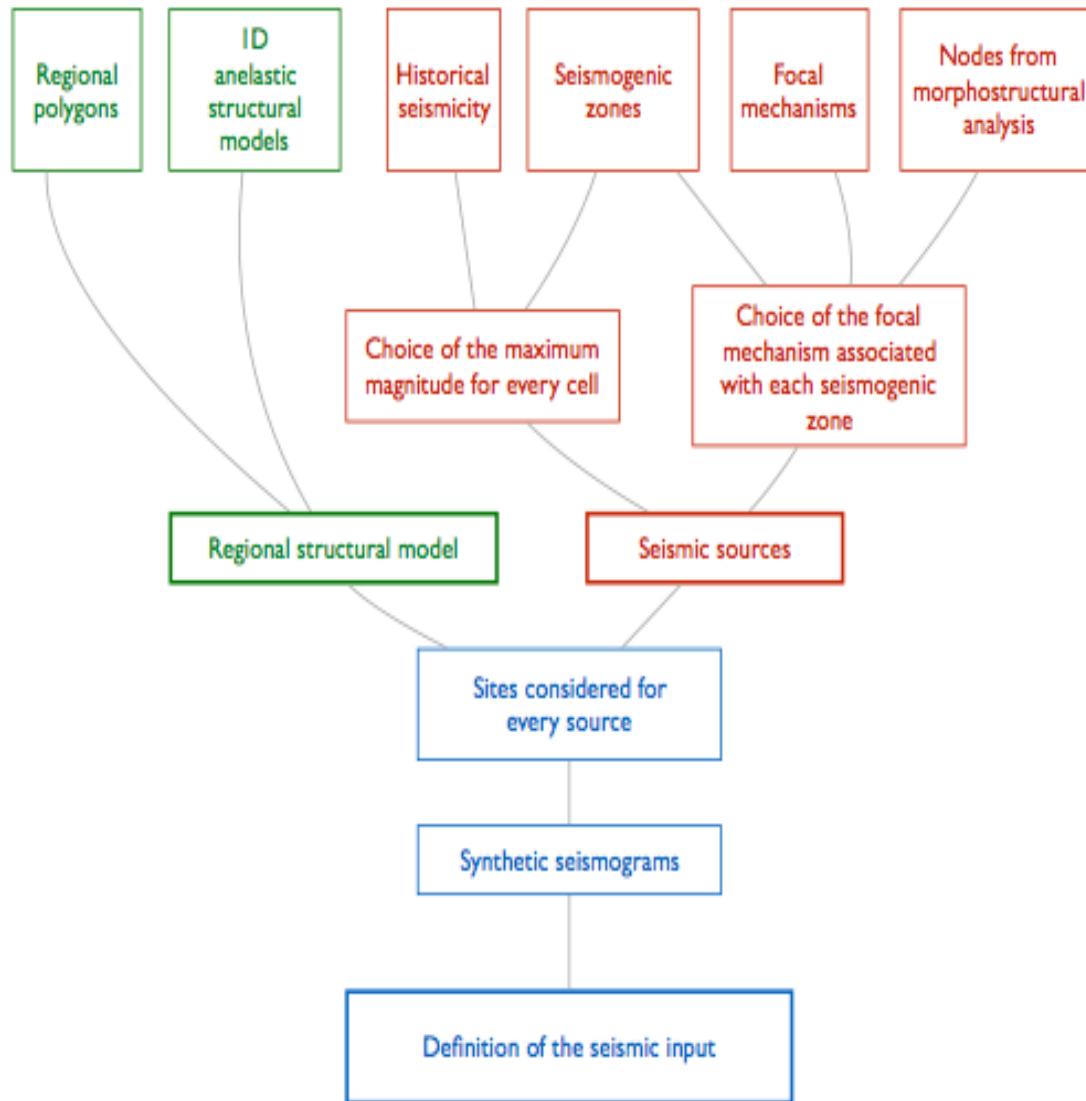


*Fig.2 Flow chart of the different steps in the NDSHA approach for the regional scale analysis.*

For national-scale seismic hazard mapping, a “Regional Scale Analysis” (RSA) is carried out using all possible seismic sources and a simplified sequel of different adjacent laterally homogeneous structural models, in welded contact, representative of bedrock conditions. When a detailed analysis is needed, to duly model the site-effects, a “Site-Specific Analysis” (SSA) can be performed (Fig.3) introducing not only the modeling of structural and topographical heterogeneities along a specific profile but also of the influence of the source rupture process on the seismic wavefield at a site. So far the NDSHA method has been applied in several countries at different levels of detail (e.g., Mourabit et al., 2014; Panza et al., 2012); Hassan et al., 2017; El-Sayed et al., 2004; Lokmer et al., 2002).

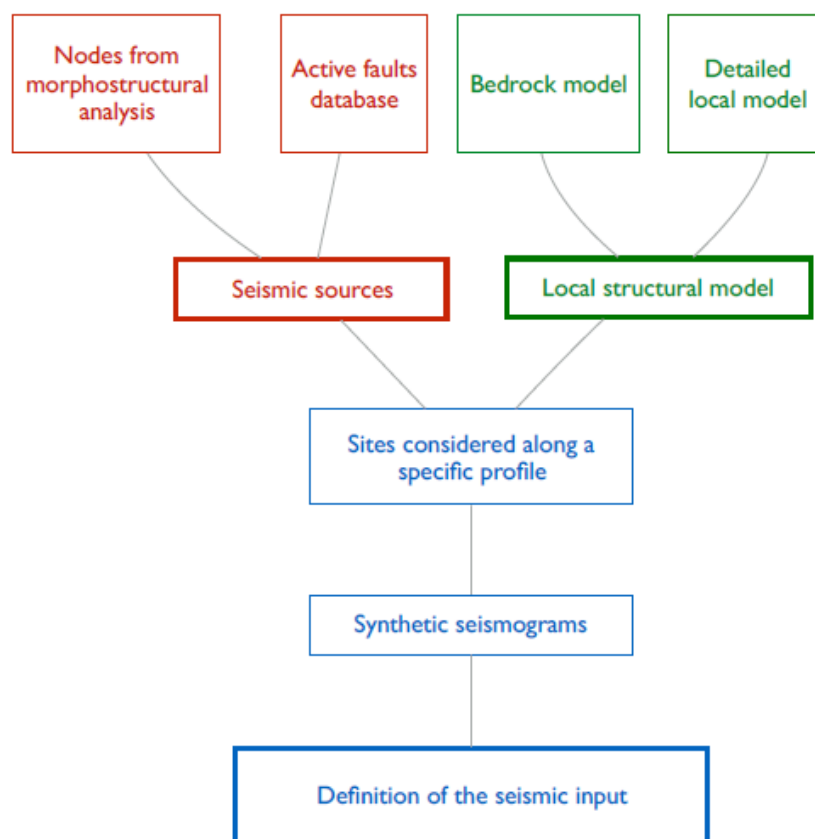


*Fig.3 Flow chart of the different steps in the NDSHA approach for the site scale analysis.*

### **3. Geology and seismicity of the study area**

The geology of El Ismailia area is dsdominated by a sedimentary succession ranging from Eocene to Quaternary, with Mid-Tertiary basalts. The geological units are shown as groups, formations and smaller lithological units according to the standard international and local stratigraphic terminology. Geologic mapping in various scales and studies have been carried out previously in the investigated area by many authors (e.g., Barakat and Aboul Eta, 1970; El Shazly et al., 1974).

Information about subsurface geology is available only for formations younger than Eocene. Eocene is made of carbonate facies of 400 to 500 m thick mostly occupied the structural tableland, and it is overlain by sands and gravels (maximum thickness 80 m) then capped by Mid-Tertiary. It is mostly exposed along the foot-hill slopes of the Cairo-Gebel Shubrawit structural depressions. In the subsurface, the Oligocene sediments extend and generally slope northwards. The Miocene at the subsurface of the study area is represented mainly by the marine sandy limestones with depth up to 140 m. Most of the faulted structural ridges are built up of this facies. It is expected that the early Pliocene sediments are of fluviomarine clays and sandy clays. They represent an aquiclude horizon for the upper layers (Fig.4). The

surface geology map shows that the site of the tunnel is covered with Nile silt and clay and unconsolidated gravel and sand which make the area susceptible to liquefaction hazards.

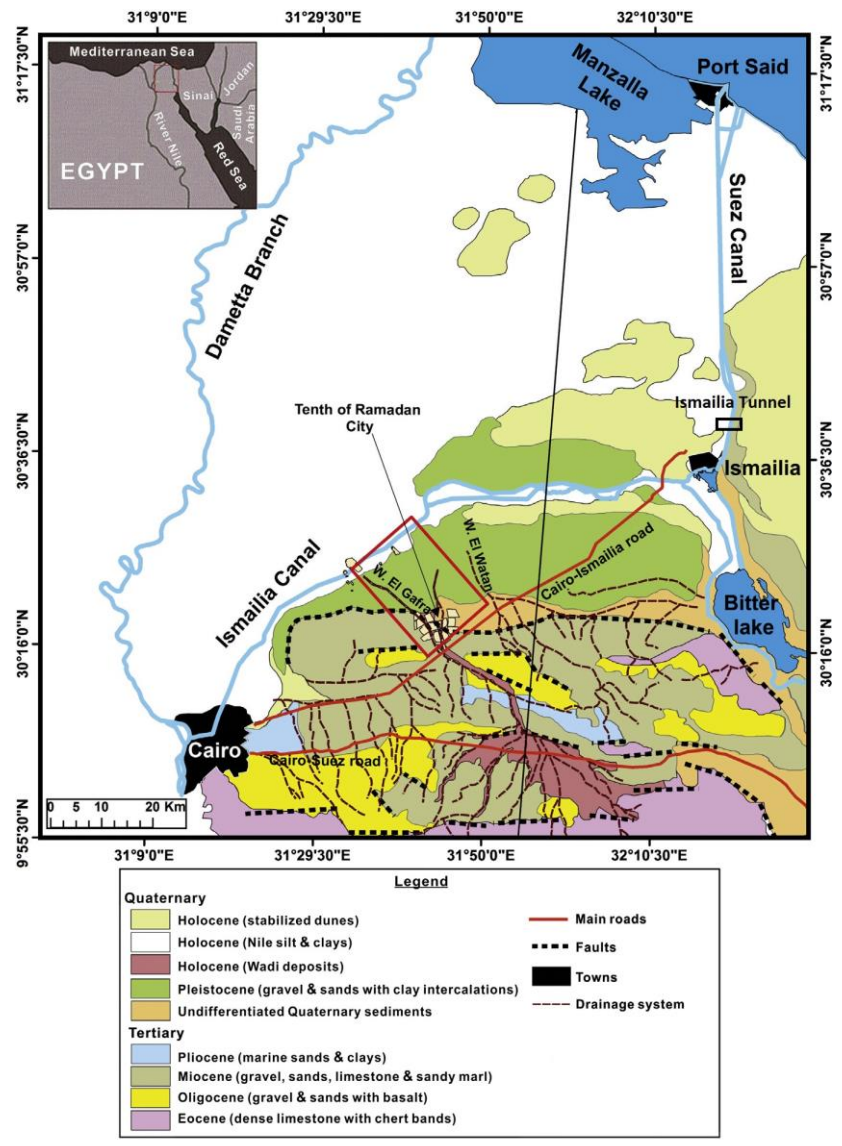


Fig.4 Geologic map of the eastern Nile Delta on which the site of the tunnel is shown (Modified after Khalil et al., 2015)

At El Qantara area, the thickness of the Early Pleistocene sediments reaches 70 to 80 m. However, no detailed studies are available for them at present. Late Pleistocene-Holocene sediments cover the area due north of Khabret Umm Gidam and the Isthmus stretch. They are characterized by the alternations of gravelly sands, sands, slightly calcareous sandstones and clays. They attain a thickness ranging from 10 to 70 m, overlying the early Pleistocene, with thickness increasing toward the north. Holocene sediments are represented by sand sheets particularly along the eastern side of the Isthmus stretch, and sand sheets and hammocks west

of El Tell El Kabir-El Salhlya plain. Sabkhas and salt marshes dominate the northern strip of El Tell El Kabir-El Salhiya plain.

According Said (1990) to Ismailia and Bitter Lakes area is affected by two major active seismic trends; Northern Red Sea-Gulf of Suez-Cairo-Alexandria-Clysmic-trend and East Mediterranean-Cairo-Fayum Pelusiatic trend. These two active seismic trends are genetically related to the well-known tectonic trends in Egypt.

Seismicity of the Suez Canal region generally and Ismailia particularly has been studied by very few studies (e.g., Hegazi et al., 2013). The seismicity map of the study area shows a sparse seismic activity around the city, along the Cairo-Suez district and Gulf of Suez rift (Fig.5). The morphostructural zonation work done by Hassan et al. (2016) has revealed a number of seismogenic nodes, which are capable of generating earthquakes of magnitude 5+ near the study site marked by a black square in Fig.5. The new data should be incorporated in any seismic hazard assessment particularly for strategic and critical structures in order to ensure the safety of such critical structures.

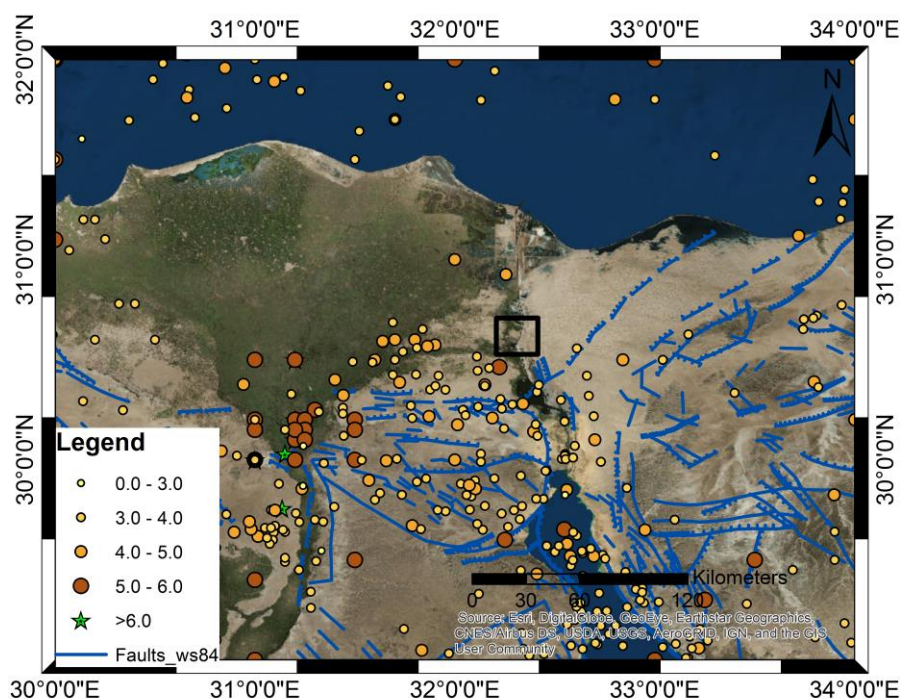


Fig.5 Seismicity of the study area. Black square defines the site of the tunnel. Blue lines are geologic faults defined by EGSMA (1981)

#### 4. Computation of $MCSI_{BD}$ at the tunnel site

The sources criteria and structural models of the Earth needed in order to perform MCSI are taken from the study of Hassan et al. (2017). The NDSHA-MCSI accommodates the

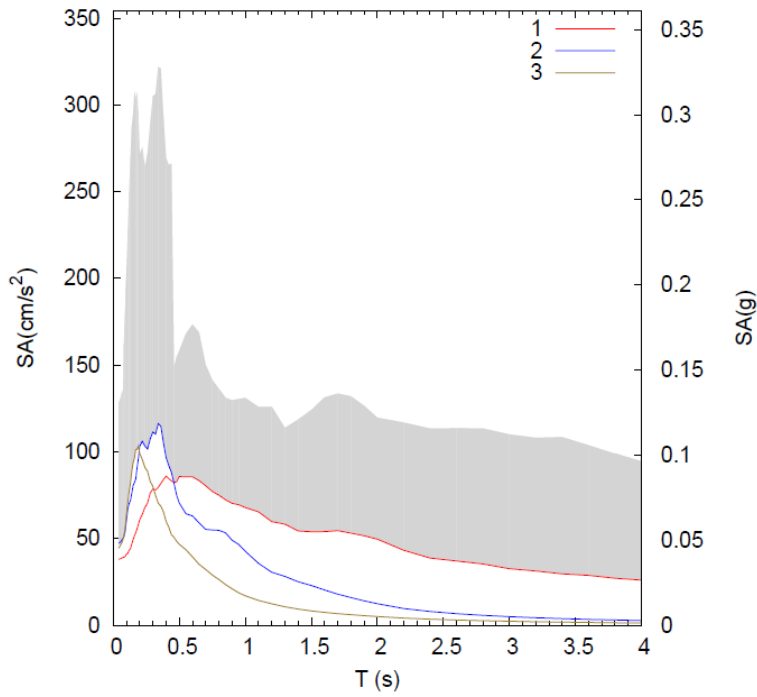


available, reliable information about the spatial distributions of the sources, their magnitudes, and focal mechanisms, as well as about the mechanical properties of the inelastic media along the transmitting pathway.

Actually, for MCSI computations dedicated to reliable engineering analyses, MCSI should be obtained using a significant number of realizations. For example, a number of 100 realizations of the rupturing process is used, which should be enough for most applications.

In this work, three-component synthetic seismograms are computed at the free surface at the new tunnel site located North of Ismailia city. The cutoff frequency is 10 Hz in the domains of displacement, velocity, and acceleration. All the potential sources, within an epicentral distance of about 300 km, have been considered taking into account changes in magnitude, rupture directivity, and fault mechanism. For those sources, parametric test has been performed considering 100 different realizations of the source rupturing process, for three directivity angles (i.e.,  $0^\circ$ ,  $90^\circ$  and  $180^\circ$ ) of two different faulting styles (unilateral and bilateral). The focal mechanisms have been adopted based on the available earthquake mechanism solutions for the study area. The MCSI has been computed by joining the statistics for all the computed scenarios for the tunnel site.

Fig.6 shows the MCSI spectrum computed at the bed rock at the site of the tunnel. The individual spectra indicate that three earthquake scenarios are controlling the spectral acceleration. Two are dominating the short period part of the RS: a seismogenic node with  $M=5.5$  and an instrumental earthquake that occurred in 1987 with  $M=5$ . The long period part is controlled by a distant earthquake scenario: the 950 earthquakes near Cairo. At this level, the MCSI represents a sort of Uniform Hazard Spectra (UHS) (Trifunac, 2012), where the hazard is identified by the maximum magnitude expected for every potential source that could affect the sites of interest. The earthquake scenarios defined at this level are used for the detailed site-specific analysis described in the next section, using the seismogenic node as a near source and the historical event as a distant source.



source	profile	$M_w$	edi (km)	depth (km)	strike (°)	dip (°)	rake (°)	sre (°)	slon (°N)	slat (°E)	
1	sz 0007	-	7.2	42.6	15.0	248	80	190	175	31.9	30.5
2	nn 1010	-	5.5	13.1	10.0	248	80	190	238	32.3	30.5
3	sz 0007	-	5.0	9.5	10.0	248	80	190	81	32.3	30.7

Fig.6  $MCSI_{BD}$  (grey areas correspond to the values between median and 95th percentile) for the site of Fig.1. Res= resultant.

### 5. Computation of $MCSI_{SSA}$ for the tunnel site

Based on the information described in section 4 about the earthquake scenarios that control the seismic hazard at the site of the tunnel, a SSA has been performed. A laterally heterogeneous profile representative of the local conditions has been composed, using data from literature and fieldwork in order to consider the site-effects and topographic characteristics on both vertical and horizontal components of the earthquake ground motions.

The earthquake scenario used for the SSA has been chosen from the disaggregation of the  $MCSI_{BD}$  response spectrum calculated with the RSA (i.e., the source-distance combination that gives the largest spectral acceleration at periods of interest) in order to optimize computational time. The controlling events, for the range of periods from 0.0 s to 4.0 s, have been found to be magnitudes 6.5-7.0 (950 earthquakes with  $M=6.5-7.0$ ) and 5.5 (seismogenic node with  $M=5.5$ ) earthquake scenarios at an epicentral distance in the range from 20 to 100 kilometers (Fig.7).

- A hybrid technique (see Fäh, 1993 and Panza et al., 2001), based on modal summation (MS) and finite difference (FD), is used to simulate the earthquake ground motion at the selected sites. The computation is made considering three earthquake scenarios, but here we present two examples, a distant earthquake scenario with Magnitude 6.5-7.0 and a seismogenic node scenario with  $M=5.5$ . The technique allows us to handle the seismogenic characteristics of the source and the properties along the pathway with full respect of the tensor nature of earthquake ground motion (Aki & Richards, 1980). Three-component synthetic seismograms are computed on the free surface along the considered profiles, with frequency content as high as 5 Hz in the domains of displacement, velocity, and acceleration. Two source models have been considered, taking into account changes in magnitude, rupture directivity, and mechanism. Parametric tests have been carried on varying the characteristic of the scenario earthquakes (e.g., focal mechanism parameters). Response spectra (RS) have been computed starting from the synthetic accelerograms, and amplifications have been estimated in terms of response spectra ratios (RSR), using the RS computed for a bedrock model as a reference.

## **5.1. Model Parameters**

In order to perform reliable synthetic seismogram computation, one has to properly model the characteristics of the source generating the seismic energy, and of the transmitting (pathway) medium.

### **5.1.1. Source**

Synthetic seismograms are computed in the scaled point-source approximation, using a double-couple of forces placed at the hypocenter defined accordingly with the known focal mechanism properties, hypocentral depth, and magnitude. Directivity effects, different rupture styles, and rupture realizations are also taken into account. Several parameters can be adjusted when generating the Source Time Functions (STF) according to the methodology proposed by Gusev (2011).

We define two earthquake scenarios (see Fig.7):

1. Historical event 935 A.D., located near the Nile Delta,  $M=6.5-7.0$ . Distance to the target area about 100 km.
2. Morphostructural zonation node, located near Ismailia,  $M=5.5$ . Distance to the target area about 20 km.



Fig.7 Earthquake scenarios and the target site.

### 5.1.2. Reference bedrock model

The seismic energy radiated from the source propagates in the bedrock model towards the local profile. The bedrock model is representative of the average structural properties between the source and the site of interest; the bedrock model is also later used as a reference model for the estimation of the amplifications along the considered profile.

The bedrock models adopted in this study are the ones that have been recently adopted for NDSHA computations at a national scale (Hassan, et al., 2017), embedding the target profile for two different scenarios (see Fig.8). The layering of the two complete bedrock models are shown in Fig.8.

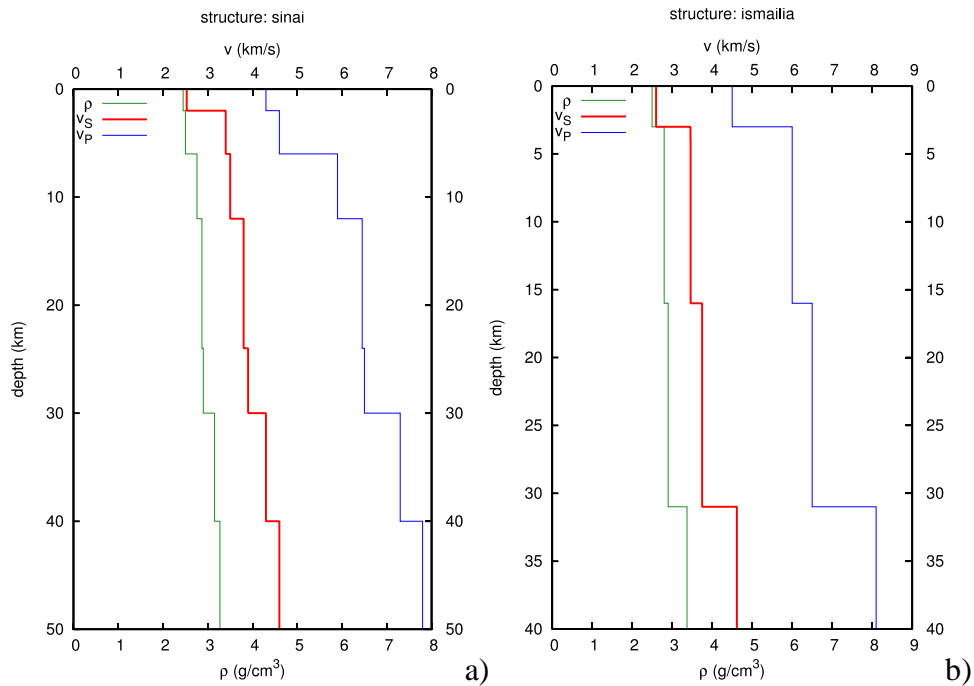


Fig.8. Reference bedrock model *Sinai* (a, for the eastern zone) and *Ismailia* (b, for the western zone).

### 5.1.3. Local Site model

This is the part of the structure corresponding to the selected sites (see Fig.9). The local model has been set up using the data from noise vibration measurements carried out along the profile and from borehole data dug near the study site, and it is shown in Fig.9. The heterogeneous part of the local structure is 10 km long and 300 m thick. Given the properties of the slowest layer considered in the local structure (260 m/s), and the highest frequency contained in the spectrum of the synthetic seismograms, the adopted grid step in this part of the model is 5 m. The FD mesh is continued at depth adopting the properties of the reference bedrock, down to a depth larger than the source depth. The grid step in this deeper and faster part of the model is 30 m. Fig.9 shows the path of the profile (top), the resulting 2-D model (middle) and the mechanical properties of the 2-D model layers together with the location of two sites selected in order to compute the seismic input at both ends of the tunnel.

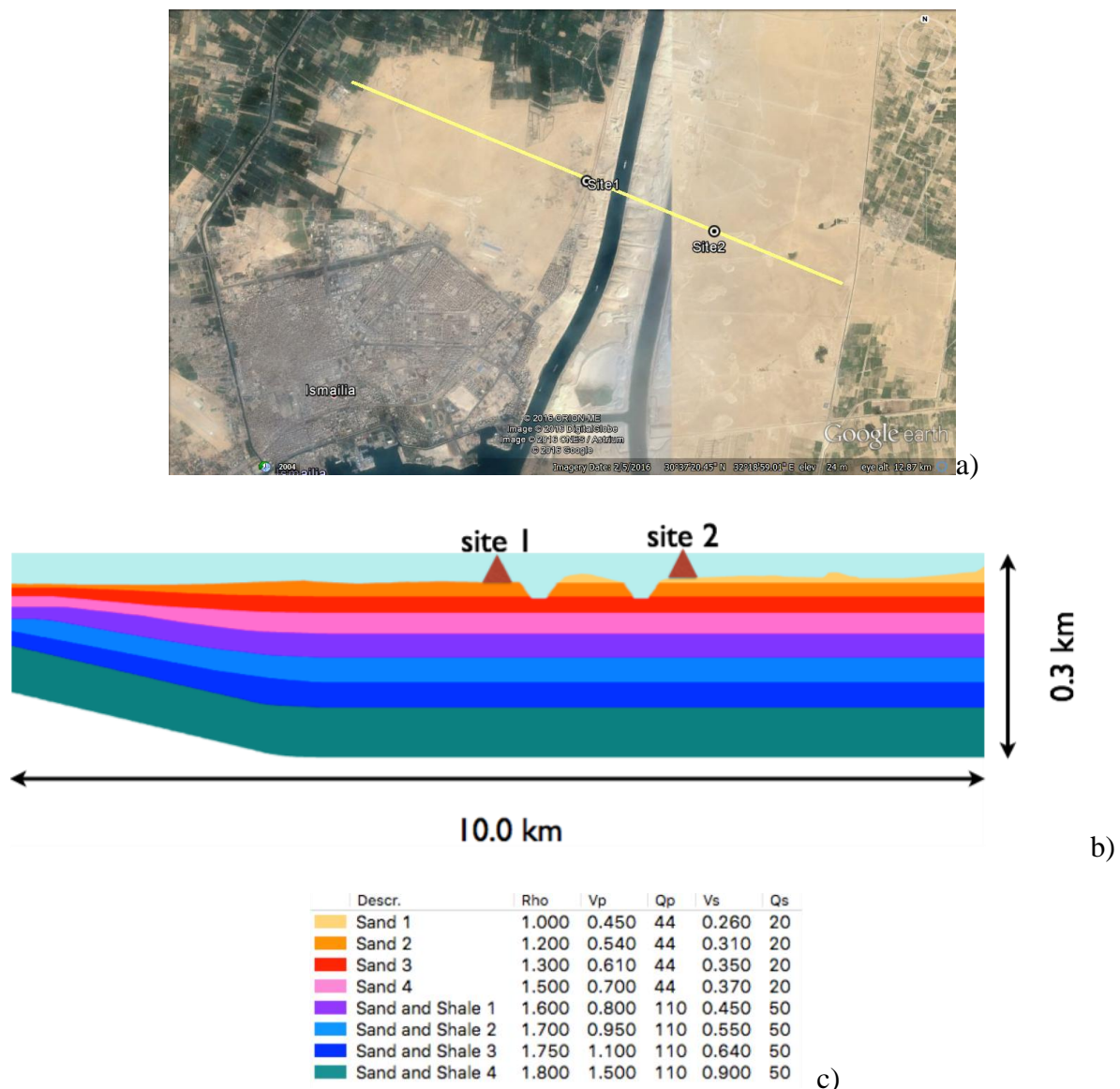


Fig.9 Target profile along the Suez Canal (a), with its section (b) and the properties of the seismological units.

## **5.2. Ground shaking scenarios**

### **5.2.1. Preliminary test**

Once defined the properties of the source, of the bedrock and of the local structure, a preliminary test is required, to confirm a) that the numerical model has been duly prepared, b) that the incoming wavefield is properly introduced in the FD mesh and c) that the unwanted reflections from the artificial boundaries of the FD model are properly removed.

The test is made creating a hybrid model where the characteristics of the bedrock are assigned also to the properties of the local structure where the FD technique is applied. Therefore we have a laterally homogeneous structural model that can be treated both with the modal summation and the finite difference techniques. The seismograms obtained with the two methods are compared, and their adequate similarity confirms that the finite difference mesh has been properly constructed.

### **5.2.2. Ground shaking for the local model: Scenario 1**

Synthetic seismograms and amplification maps for the local model and Scenario 1 are shown in Figs.10 and 11, respectively. The amplification is generated by the presence of the thin low-velocity sediments on top of the model. Velocities and displacements, having relatively less energy in the high-frequency part of the spectrum, are less influenced by the presence of the thin topmost layers.

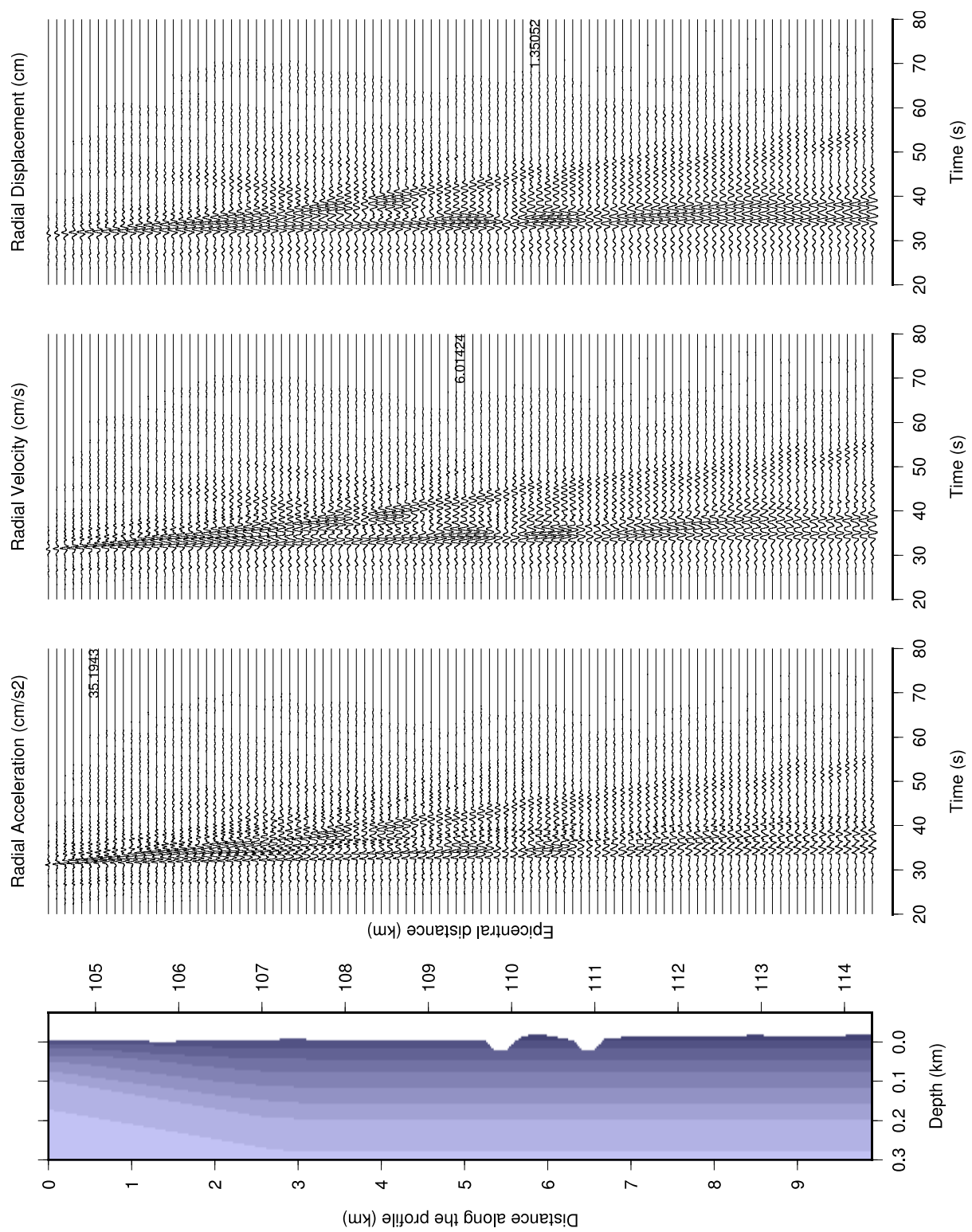


Fig.10a Radial component synthetic seismograms along the profile. Accelerations in  $\text{cm/s}^2$ , velocities in  $\text{cm/s}$ , displacements in  $\text{cm}$ .

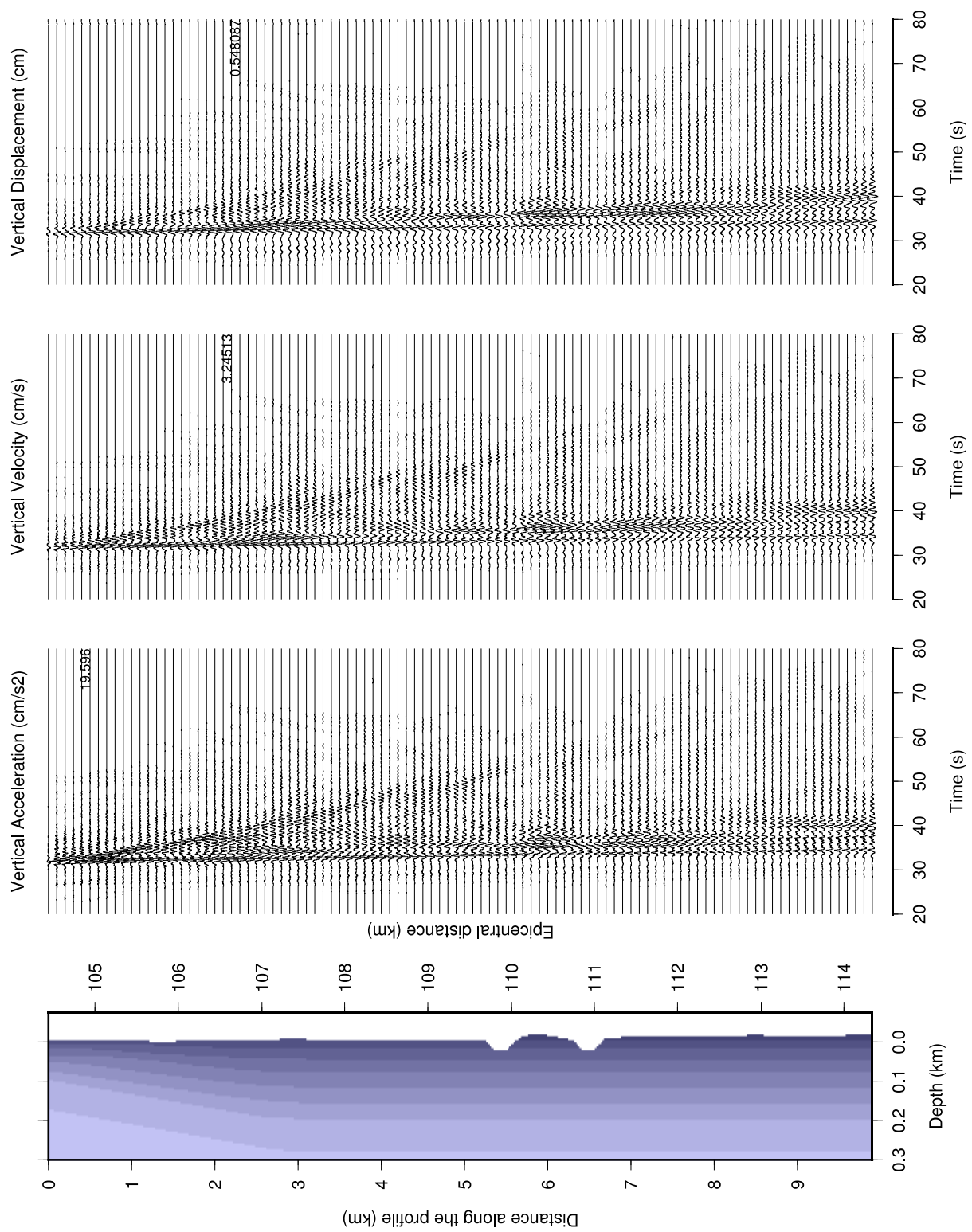


Fig.10b Vertical component synthetic seismograms along profile. Accelerations in  $\text{cm/s}^2$ , velocities in  $\text{cm/s}$ , displacements in  $\text{cm}$ .



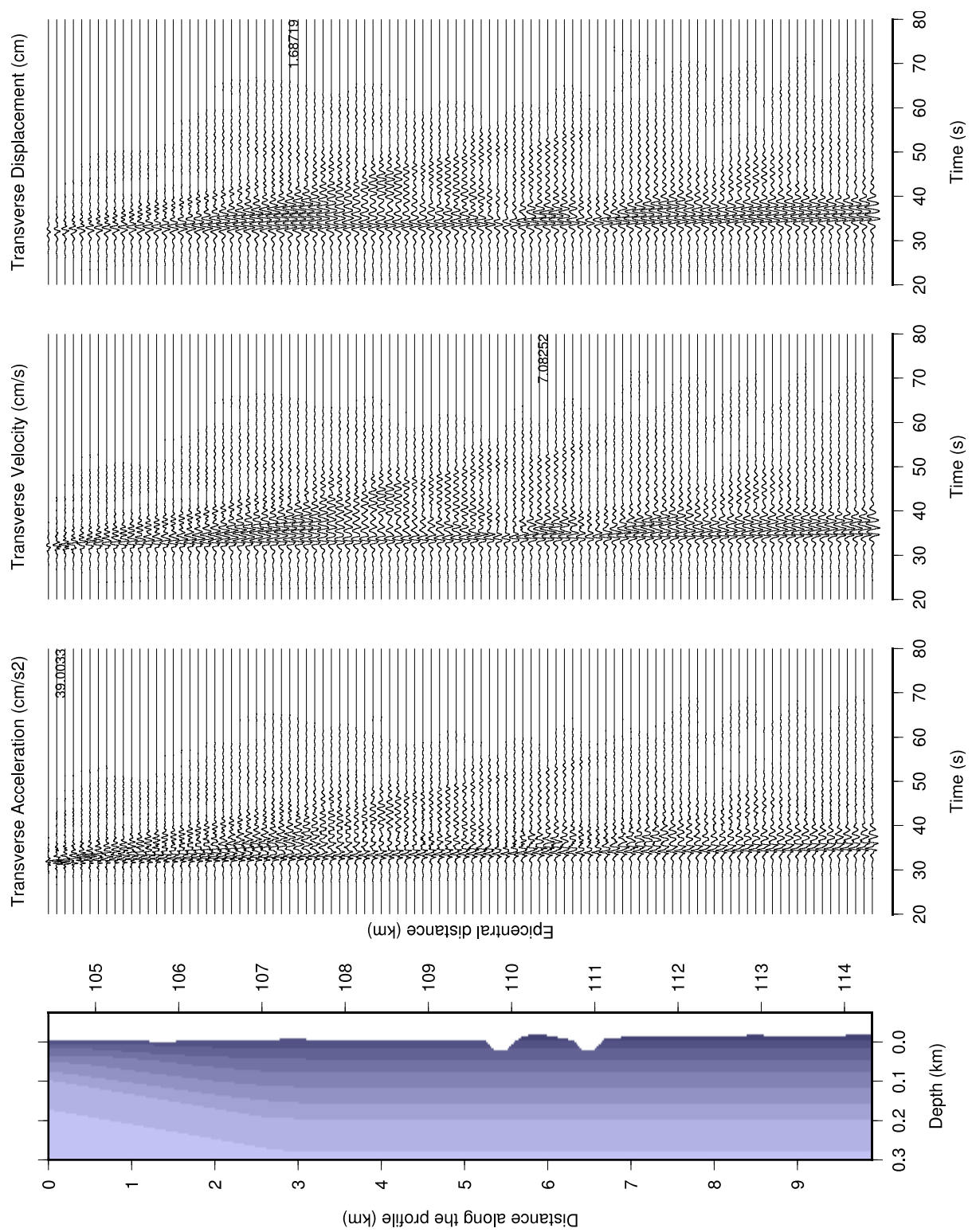


Fig.10c Transverse component synthetic seismograms along the profile. Accelerations in  $\text{cm/s}^2$ , velocities in  $\text{cm/s}$ , displacements in  $\text{cm}$ .

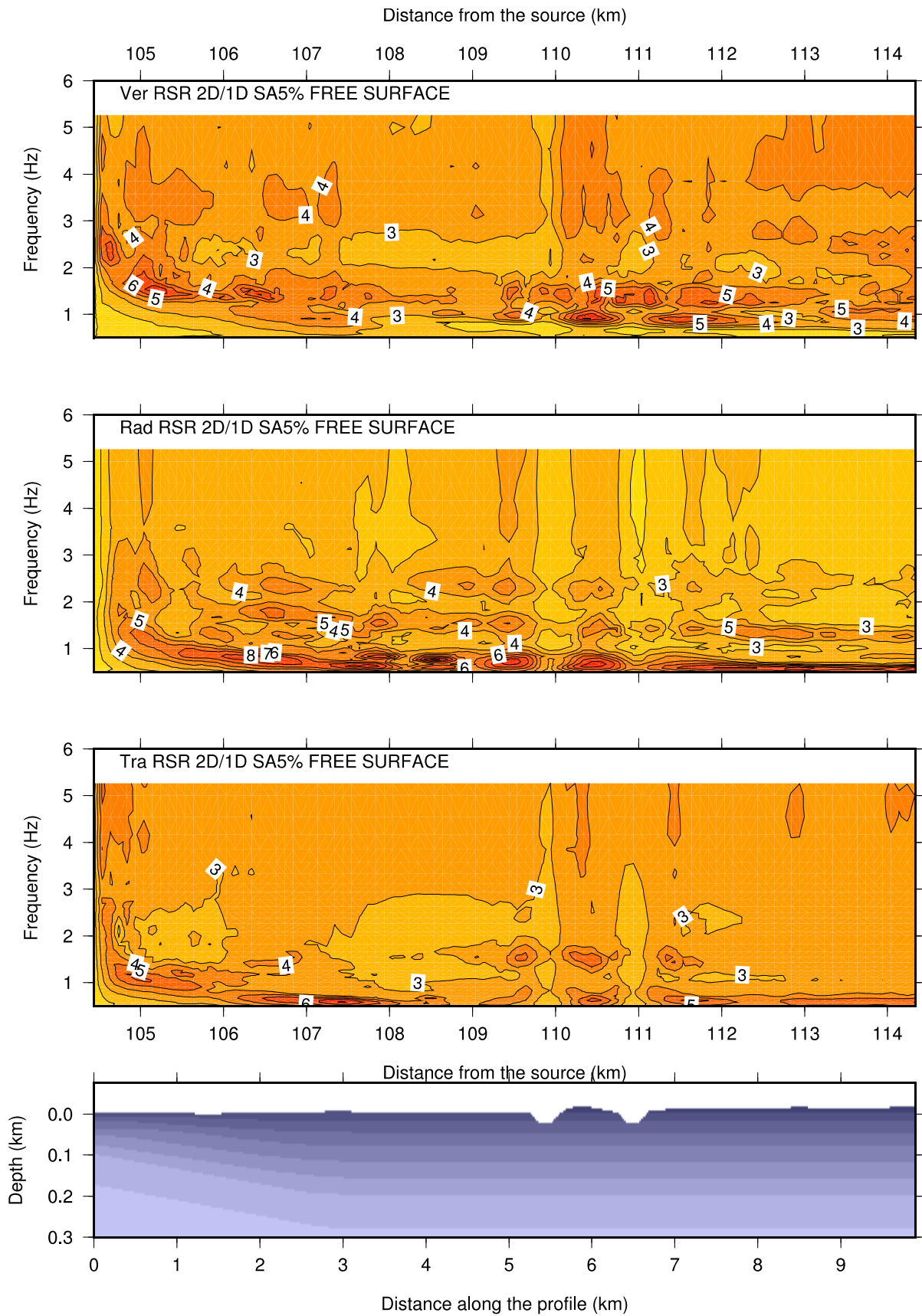


Fig.11 Amplification pattern for the profile (RSR/Ismailia).

### 5.2.3. Ground shaking for the local model: Scenario 2

Synthetic seismograms and amplification maps for the local model and Scenario 2 are shown in Figs.12 and 13, respectively.

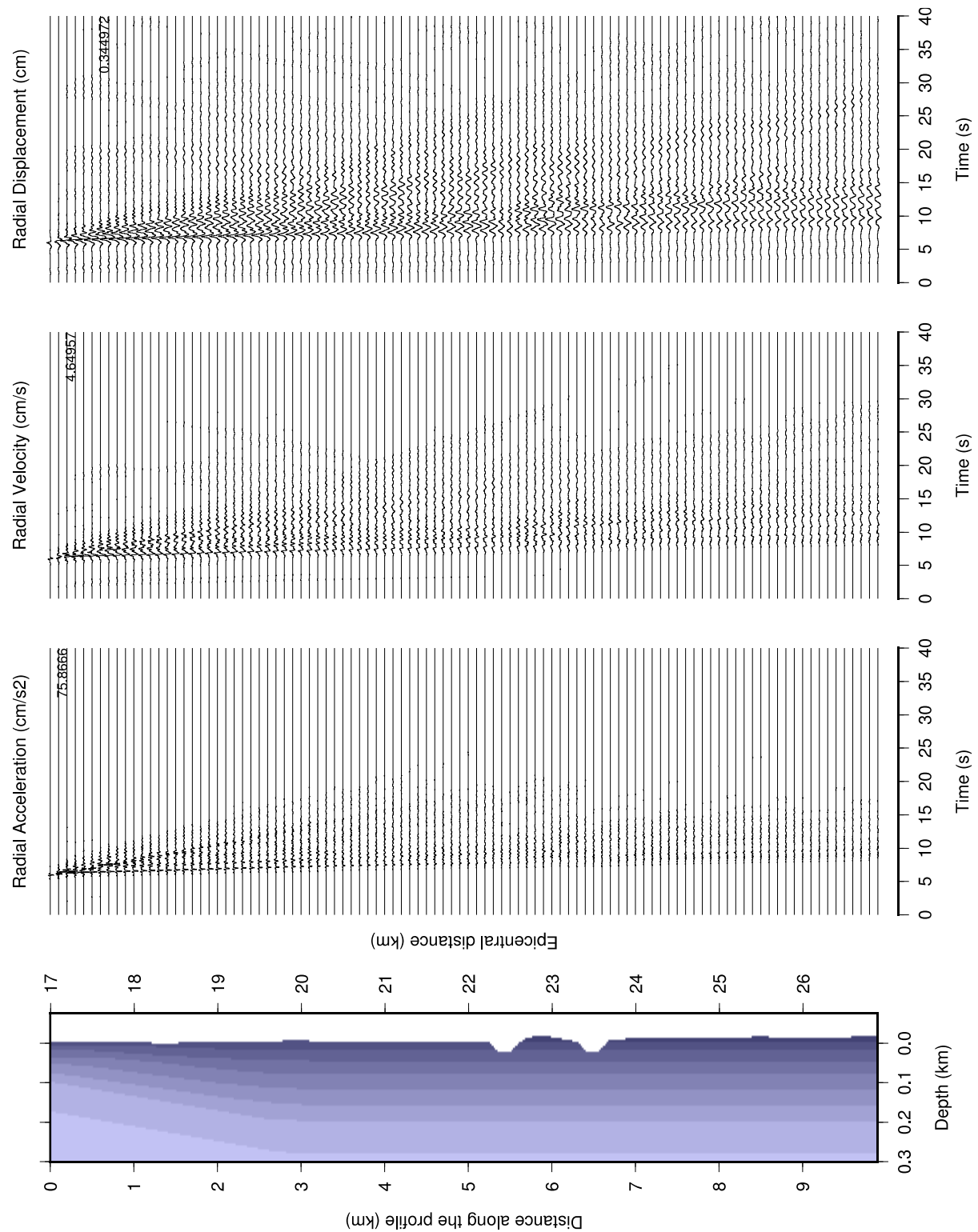


Fig.12a Radial component synthetic seismograms along the profile. Accelerations in  $\text{cm/s}^2$ , velocities in  $\text{cm/s}$ , displacements in  $\text{cm}$ .

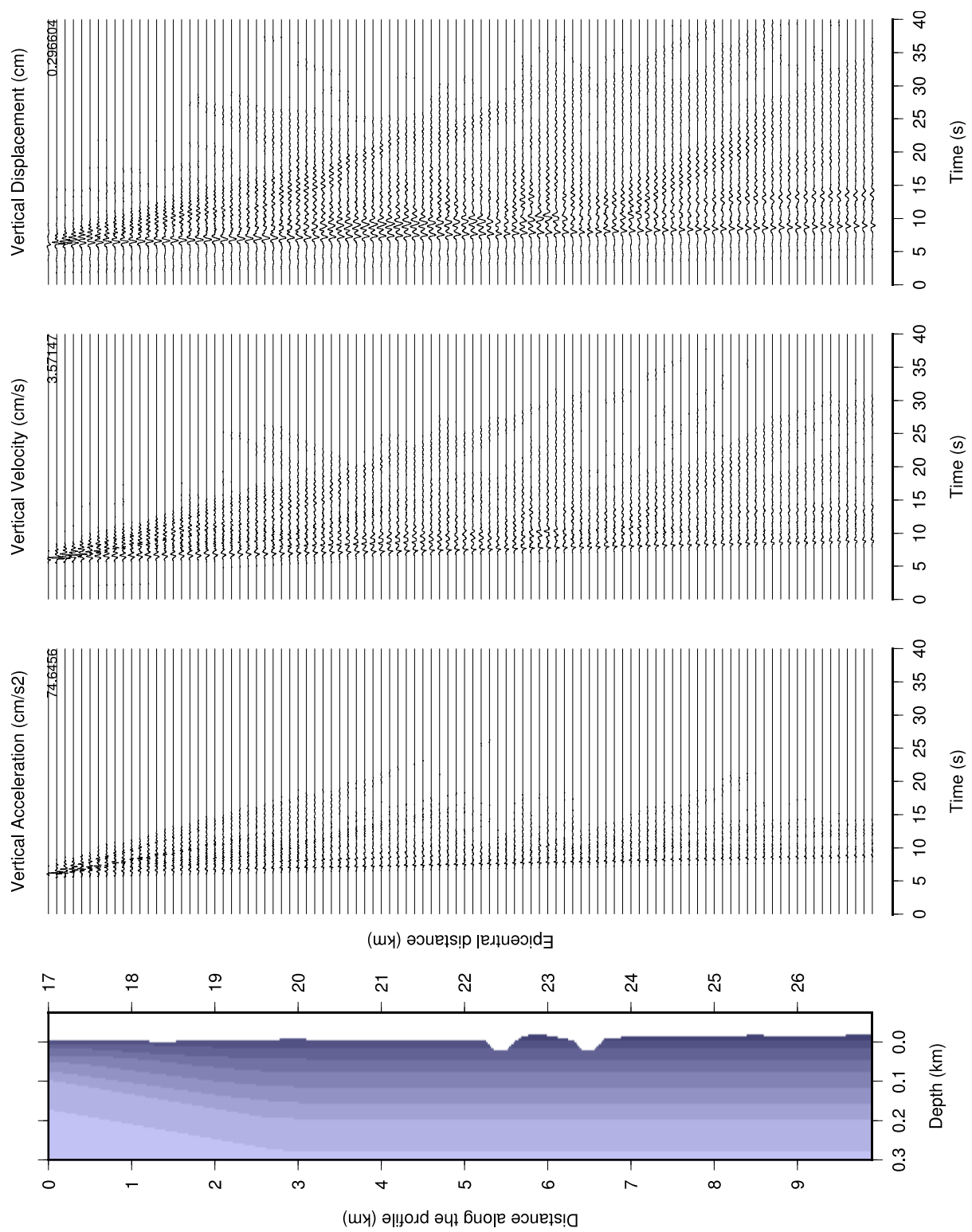


Fig.12b Vertical component synthetic seismograms along profile. Accelerations in  $\text{cm/s}^2$ , velocities in  $\text{cm/s}$ , displacements in  $\text{cm}$ .

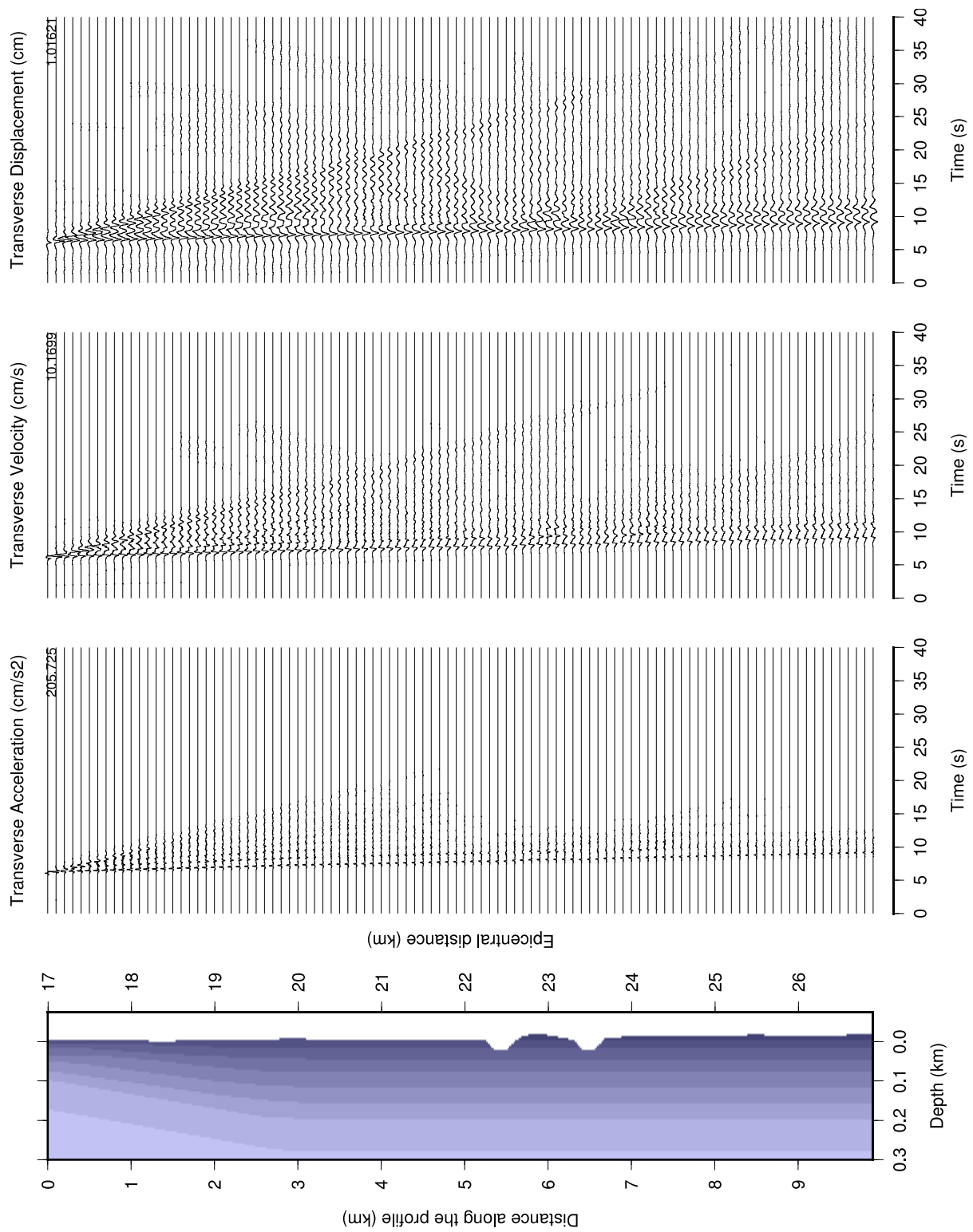


Fig.12c Transverse component synthetic seismograms along the profile. Accelerations in  $\text{cm/s}^2$ , velocities in  $\text{cm/s}$ , displacements in  $\text{cm}$ .

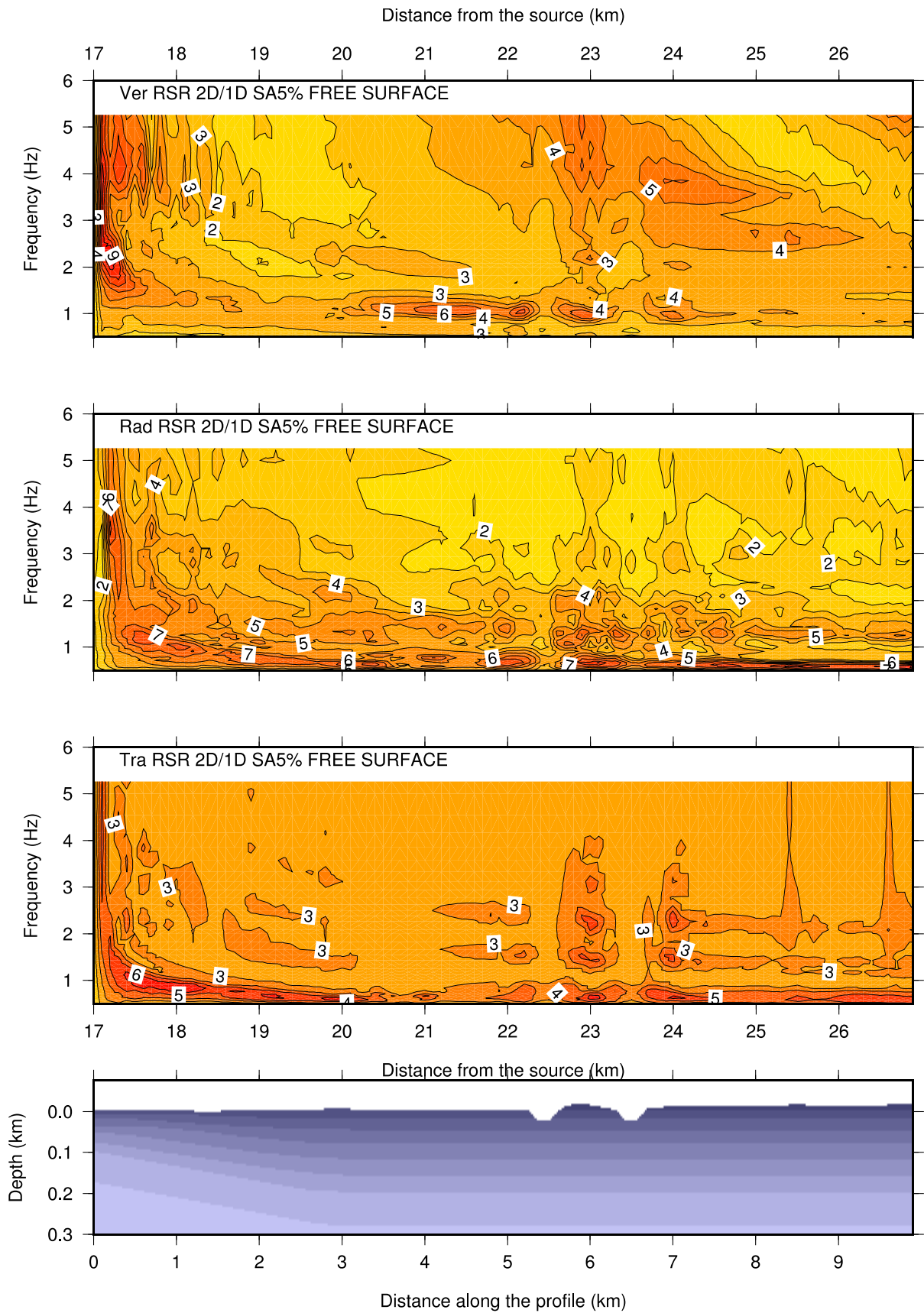


Fig.13 Amplification pattern for the profile (RSR/Ismailia).

## 6. Discussion and conclusions

- NDSHA brings the balance in the pursuit of realistic seismic hazard as in the areas where lacking ground motion records and sparse seismicity; the method could accommodate information from different techniques including; Geologic, Tectonic, and Morphostrucral information as well as account for their uncertainty.
- The calculated Response spectra could reflect that it is impossible to use only the worst case scenario to account for all expected spectrum. The complex nature of expected ground motion will not survive unless including different sources with different realization and keeping the tensor nature of the problem that holds the directivity nature and site effect.

Starting from the initial definition of the source, bedrock and site properties, based on the available knowledge of the characteristics of the two earthquake scenarios and of the structural properties of the area, a set of ground shaking scenarios have been computed at the selected profile go across the Suez Canal.

Modifications of the ground shaking scenarios have to be evaluated looking basically a) at the amplitudes measured on the waveforms and the response spectra, b) at the changes in the duration of the shaking, and c) at the modifications to the amplification patterns.

To compare how the two source configurations can modify the seismic input we compare (see Fig.14 (a and b)) the response spectra computed at the two selected sites (shown in Figure 7.a and b). For each site, the curves show the effect of the combination of magnitude, distance and rupture process and how long periods are dominated by more distant, but with larger magnitude, Scenario 1 while periods shorter than 1 s are dominated by Scenario 2.

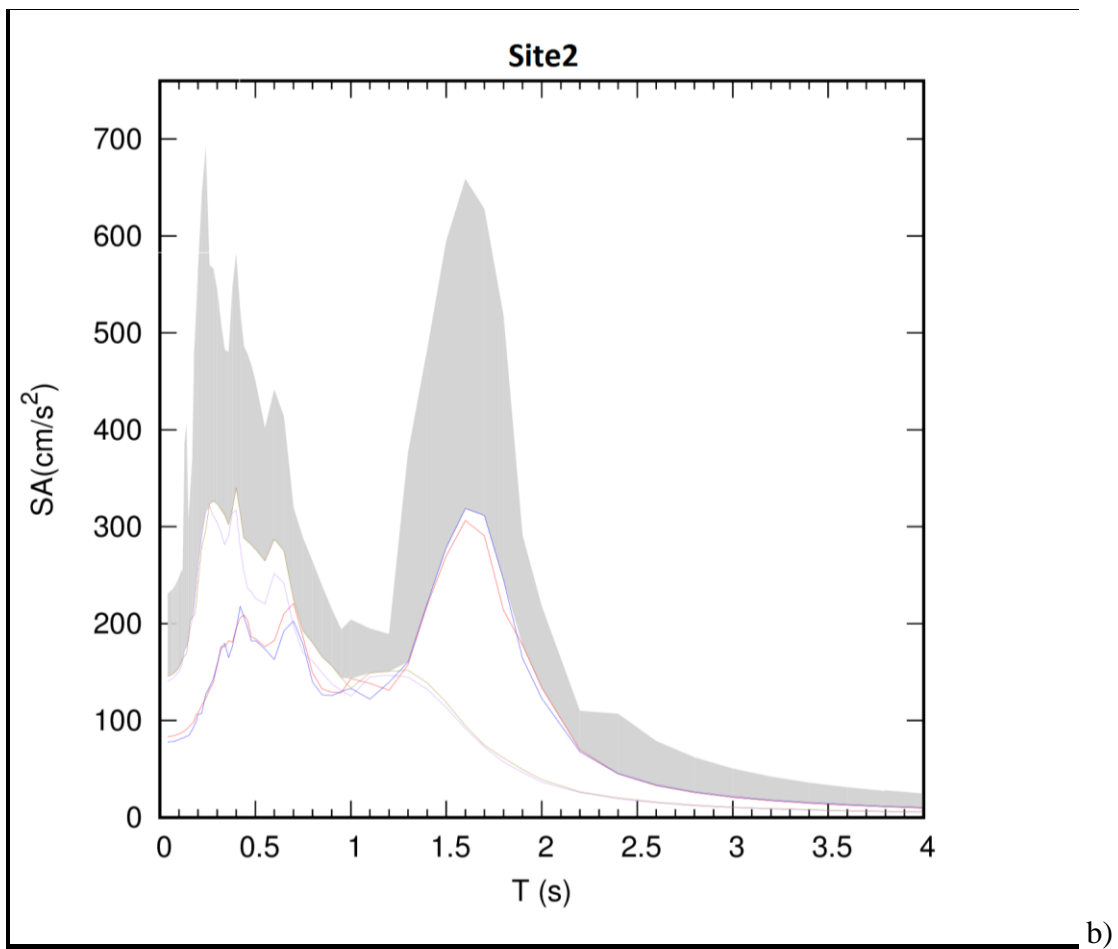
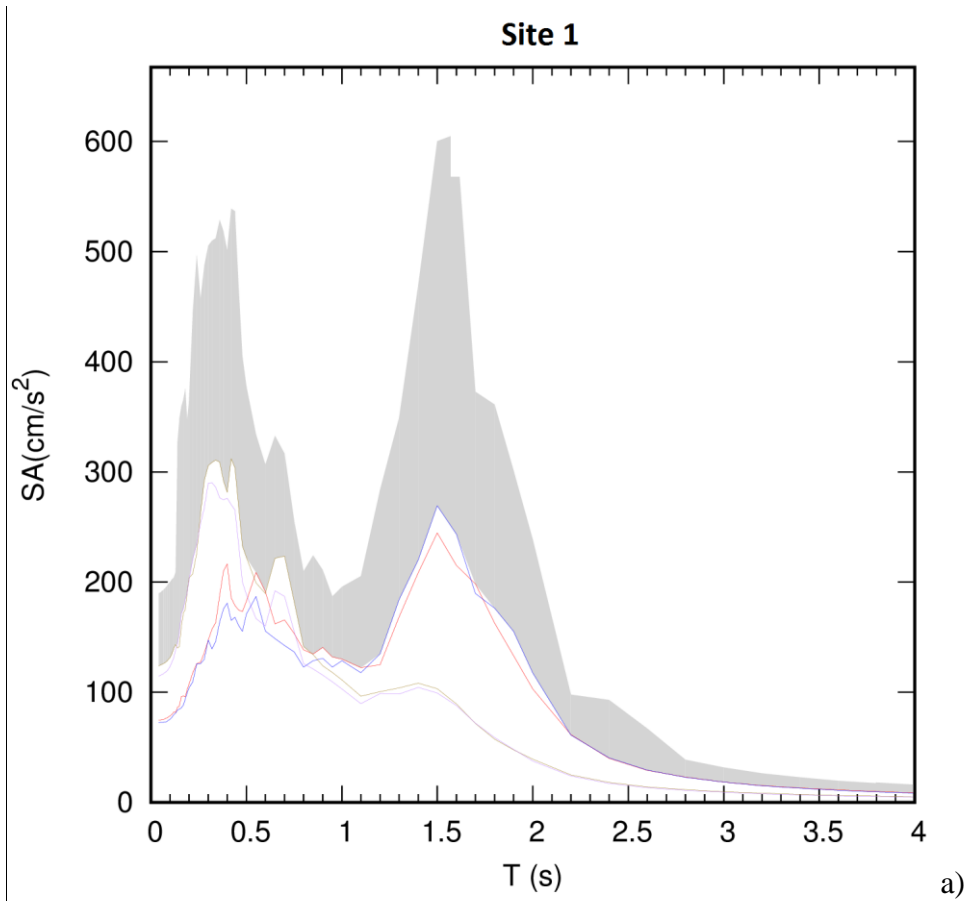




Fig.14 Response spectra computed at the two selected sites (a and b, corresponding to 1 and 2 in Fig.7 a and b) along the profile crossing the Suez Canal, for the Scenario 1 and 2.

## REFERENCES

- Aki, K., & Richards, P. G. (1980). *Quantitative Seismology: Theory and methods*. San Francisco: W.H. Freeman.
- Barakat, M.G. and About Ela, N.M. (1970) Microfacies and Paleocology of Middle Eocene and younger sediments in Geneifa area, Cairo-Suez district UAR J. Geol. 14, 23.
- El-Sayed, A., Vaccari, F., & Panza, G. F. (2004). The Nile Valley of Egypt: a major active graben that magnifies seismic waves. *Pure and applied geophysics*, 161(5), 983-1002.
- EGSMA (Egyptian Geological Survey and Mining Authority) (1981) Geologic map of Egypt 1:2000000. Ministry of Industry and Mineral Resources, Cairo, Egypt
- El Gezeery, M.N., and Marzouk, I.M. (1974) Miocene rock-stratigraphy of Egypt, Stratigraphic Subcommittee of the National Committee of Geological Sciences, Egypt. J. Geol. 18, 1.
- El-Shazly, E. M., A'adel Hady, M.A. El Ghawaby, M.A., El Kassas, I.A. and El Shazly, M.M. (1974) "Geology of Sinai Peninsula from ERTS-1 satellite images" Remote Sensing Research Project, Academy of Scientific Research and Technology, Cairo, Egypt.
- Fäh, D., Iodice, C., Suhadolc, P., & Panza, G. F. (1993). A new method for the realistic estimation of seismic ground motion in megacities: the case of Rome. *Earthquake Spectra*, 9(4), 643-668.
- Fasan, M., Amadio, C., Noè, S., Panza, G., Magrin, A., Romanelli, F., & Vaccari, F. (2015). A new design strategy based on a deterministic definition of the seismic input to overcome the limits of design procedures based on probabilistic approaches. In XVI ANIDIS Conference, L'Aquila, Italy. arXiv preprint arXiv:1509.09119.
- Fasan, M. (2017). Advanced seismological and engineering analysis for structural seismic design. Ph.D. thesis, Trieste University – Italy.
- Gusev, A.A. (2011) Broadband kinematic stochastic simulation of an earthquake source: a refined procedure for application in seismic hazard studies. *Pure Appl. Geophys.* 168, 155–200. doi:10.1007/s00024-010-0156-3.
- Hegazi, A. M., Seleem, T. A., & Aboulela, H. A. (2013). The Spatial and Genetic Relation between Seismicity and Tectonic Trends, the Bitter Lakes Area, North-East Egypt. *Geoinfor Geostat: An Overview 1: 2. of, 7, 2.*
- Hassan, H. M., Romanelli, F., Panza, G. F., ElGabry, M. N., & Magrin, A. (2017). Update and sensitivity analysis of the neo-deterministic seismic hazard assessment for Egypt. *Engineering Geology*, 218, 77-89.
- Hassan, H. M., Panza, G. F., Romanelli, F., & ElGabry, M. N. (2017). Insight on seismic hazard studies for Egypt. *Engineering Geology*, 220, 99-109.
- Hassan, H. M., Gorshkov, A., Novikova, O. V. (2016, April). Recognition of seismogenic nodes ( $M > 5.0$ ) in north-east of Egypt. The African Seismological Commission 1st general Assembly, Luxor, Egypt.
- Khalil, M. M., Tokunaga, T., & Yousef, A. F. (2015). Insights from stable isotopes and hydrochemistry to the Quaternary groundwater system, south of the Ismailia canal, Egypt. *Journal of Hydrology*, 527, 555-564.
- Lokmer, I., Herak, M., Panza, G. F., & Vaccari, F. (2002). Amplification of strong ground motion in the city of Zagreb, Croatia, estimated by computation of synthetic seismograms. *Soil Dynamics and Earthquake Engineering*, 22(2), 105-113.
- Magrin, A., Gusev, A. A., Romanelli, F., Vaccari, F., & Panza, G. F. (2016). Broadband NDSHA computations and earthquake ground motion observations for the Italian territory. *International Journal of Earthquake and Impact Engineering*, 1(1-2), 131-158.
- Mourabit, T., Elenean, K. A., Ayadi, A., Benouar, D., Suleman, A. B., Bezzeghoud, M., ... & Hfaiedh, M. (2014). Neo-deterministic seismic hazard assessment in North Africa. *Journal of seismology*, 18(2), 301-318. <http://dx.doi.org/10.1007/s10950-013-9375-2>.

- Molchan G., Kronrod T. and Panza F., (2011). Hot/Cold Spots in Italian Macroseismic Data. *Pure Appl. Geophys.* Vol 168, pp. 739-752; doi: 10.1007/s00024-010-0111-3.
- Panza, G. F., Romanelli, F., & Vaccari, F. (2001). Seismic wave propagation in laterally heterogeneous anelastic media: theory and applications to seismic zonation. *Advances in geophysics*, 43, 1-95.
- Panza, G. F., La Mura, C., Peresan, A., Romanelli, F., & Vaccari, F. (2012). Chapter three-seismic hazard scenarios as preventive tools for a disaster resilient society. *Advances in geophysics*, 53, 93-165.
- Said R (1990) *The geology of Egypt*. A.A. Balkema, Rotterdam.
- Trifunac, M.D., 2012. Earthquake response spectra for performance based design-A critical review. *Soil Dynamics and Earthquake Engineering* 37, 73–83. doi:10.1016/j.soildyn.2012.01.019
- Zuccolo, E., Vaccari, F., Peresan, A., & Panza, G. F. (2011). Neo-deterministic and probabilistic seismic hazard assessments: a comparison over the Italian territory. *Pure and Applied Geophysics*, 168(1-2), 69-83.